Heat capacity of gadolinium near the Curie temperature

Grzegorz Bednarz
Department of Chemistry, Dalhousie University, Halifax, Canada B3H 4J3

D. J. W. Geldart
Department of Physics, Dalhousie University, Halifax, Canada B3H 3J5

Mary Anne White*
Department of Chemistry, Dalhousie University, Halifax, Canada B3H 4J3
(Received 10 December 1992; revised manuscript received 26 February 1993)

High-resolution ac calorimetric data near the Curie point are reported for several single crystals of gadolinium. The critical temperature and the shape of the heat-capacity curve near T_c both depend on the sample-preparation procedure, including heat treatments. The heat-capacity data are analyzed in terms of predictions of renormalization-group theory. This analysis shows that the critical behavior of Gd is consistent with the picture of a complex critical behavior consisting of a series of crossovers dictated by the interplay between short-range and magnetic-dipolar interactions.

I. INTRODUCTION

Measurements of the heat capacity represent a well-established method of studying phase transitions. The progress made in the physics of critical phenomena in the two decades since Wilson[1] formulated the renormalization-group (RG) approach to phase transitions in 1971 has intensified the need for data giving the temperature dependence of the heat capacity, $C(T)$, at temperatures extremely close to the critical value, T_c. The required heat-capacity resolution can be of the order of a few mK, in order to give reduced temperatures, $t=(T-T_c)/T_c$, less than 10^{-3}. Such high-resolution heat-capacity data can be used for testing and further development of existing RG models of phase transitions.

The present study involves high-resolution measurements of the isobaric heat capacity for several samples of single crystals of Gd near the Curie point. The critical behavior of Gd has attracted a good deal of attention recently. The recent results of the studies of the critical behavior of Gd are reviewed in Sec. II of this paper. A brief account of the experimental method, which involves the application of ac calorimetry for high-resolution measurements and the description of the sample preparation procedures, including different heat treatments, is given in Sec. III. The results of the heat-capacity measurements are given in Sec. IV and the data analysis is presented in Sec. V. The results are discussed in Sec. VI and summarized in Sec. VII.

II. THE CASE OF GADOLINIUM

A. Magnetic structure

Gadolinium (Gd) is one of the simpler heavy rare-earth metals and it exhibits a ferromagnetic phase transition at around 295 K.[2-4] The crystalline structure of Gd is hexagonal close packed with a unit-cell c/a ratio of about 1.59 near T_c, which is close to the ideal value of $c/a=(8/3)^{1/2}\approx 1.63$.

Gadolinium may be expected to exhibit only weak single-ion anisotropy, since its magnetism is produced almost wholly by spherically symmetric $^8S_{7/2}$ ions. (The electron configuration of Gd is $4f^7 5d^1 6s^2$; the large magnetic moment of Gd is localized in the $4f$ shell and the effective Bohr magneton number in the paramagnetic region is around 8.[5]) There is also a small conduction electron contribution to the total magnetism which can be treated as a polarization of spins of conduction electrons induced by the $4f$ moments.

Below T_c the easy direction of magnetization is temperature dependent. Magnetization measurements,[5,6] neutron diffraction,[7] and crystalline anisotropy[8] show that the angle between the c axis and the easy axis increases from around 30° at 10 K to around 65° at 183 K and drops abruptly to zero at $T\approx 232$ K. In the range of the present study, the unique direction of magnetization is thus the c axis.

B. Static critical exponents

The critical behavior of gadolinium is not yet fully understood.[4,9,10] On the one hand, the S-state nature of the Gd moments coupled by isotropic Ruderman-Kittel-Kasuya-Yosida interactions suggests Heisenberg critical behavior near T_c. On the other hand, the unique easy (c-axis) direction of magnetization implies uniaxial anisotropy, which suggests Ising critical behavior sufficiently close to T_c. Static critical exponent measurements span predictions of both the models.[4]

Values of the critical exponent β cluster around 0.39 and support the Heisenberg critical behavior.[4,11,12] The exponent for the magnetic susceptibility, γ, is typically found to be near the three-dimensional Ising value ($\gamma\approx 1.24$),[13-16] while values of δ are generally too low for either prediction.[11,12]

0163-1829/93/47(21)/14247(13)/$06.00

Literature values of the critical exponent α for Gd have been obtained from heat-capacity measurements by ac calorimetry[17–19] continuous warming calorimetry,[20,21] and from thermal-expansion measurements.[20,22] The values of α suggest Heisenberg behavior by their sign, but are generally much larger in magnitude than the theoretical value.

Under the constraint that $\alpha=\alpha'$ Lanchester *et al.*[20] were able to obtain a good power-law fit to their heat-capacity data for a single crystal of Gd only after allowing for a discontinuity at T_c ($\alpha=\alpha'=-0.30$ from this fit). They also had to allow for a discontinuity at T_c in order to obtain a good power-law fit to the c-axis thermal-expansion data for another Gd single crystal of comparable quality ($\alpha=\alpha'=-0.32$ from this fit).[20]

Dolejsi and Swenson[22] made thermal-expansion measurements on a single crystal of Gd over several decades of reduced temperature ($10^{-5}<|T_c|<10^{-1}$) and could not find a single power-law representation for their data even after restricting the fits to temperatures only just above or just below T_c. Dolejsi and Swenson had to use four reduced-temperature ranges to represent their data by power-law fits (correction to scaling terms were not included in their fits). Above T_c the division point was selected at the reduced temperature $t=1.3\times10^{-3}$. Above that temperature $\alpha=-0.121$, agreeing well with that predicted for the three-dimensional (3d) Heisenberg model (-0.115 ± 0.009).[23] For $t<1.3\times10^{-3}$ the value of α was -1.71, an unrealistically large negative number suggesting that the data should be fit to another model very close to T_c.

Inconsistency between the measurements leads to disagreement between theory and experiment, including the apparent violation of scaling laws such as $\alpha+2\beta+\gamma=2$. There can be several causes for the inconsistency. Nonasymptotic data can lead to widely different values of critical exponents, depending on the temperature range of the fit. The quality of a crystal also affects results: The presence of impurities or defects may lead to an entirely new critical behavior. Finally, the critical behavior of a real system may not be simple, but it may change depending on the distance from T_c (in the reduced temperature scale), exhibiting a pattern of overlapping crossovers. In such a case, analysis of data in terms of power laws will generally yield effective exponents even though corrections to asymptotic scaling are included.

C. Uniaxial anisotropy in Gd

A characteristic feature of uniaxial systems with both magnetic dipolar and exchange interactions is that the heat capacity appears to have a discontinuity at T_c, similar to that observed for Gd.[24–26] In these systems the critical behavior is represented by mean-field laws modified by fractional powers of the logarithm of the reduced temperature, t.[27,28] Because the logarithmic corrections become important only very close to the critical temperature, the critical behavior of these systems strongly resembles the classical Landau behavior. This is reflected in the power-law fits which indicate the presence of a discontinuity at T_c.

The suggestion that magnetic dipolar interactions may be important for understanding the critical behavior of Gd was made in 1975 by Geldart and Richard.[29] In 1987 Geldart *et al.*[9] reported measurements of the electrical resistivity of a c-axis single crystal of high-purity gadolinium metal in the vicinity of the Curie temperature ($|t|<10^{-3}$). Numerical analysis showed that the data could not be well described by a power law of the type expected for short-range interactions and tended to exhibit a change in effective slope at T_c. Good fits were obtained when the data were described in terms of logarithmic corrections to the regular term of the sort expected for a uniaxial dipolar system.

Anisotropy in the critical properties of Gd was seen in the work of Collins, Chowdhury, and Hohenemser[30] on perturbed $\gamma\gamma$ angular-correlation experiments on a single crystal of Gd above T_c. Models of critical dynamics based on isotropic spin fluctuations did not give good results for $t<10^{-3}$. However, their experimental results for $t<10^{-3}$ were well described by an anisotropic spin-fluctuation model.

Further evidence for the uniaxial anisotropy in Gd was provided by Geldart *et al.*,[10] in measurements of the magnetic susceptibility along the c axis and in the basal plane on a single crystal of Gd in the reduced temperature range $4\times10^{-4}<t<1.3\times10^{-2}$. They observed that the basal plane (hard direction) susceptibility, χ_b, remained finite at T_c and extrapolated to zero at a temperature which was below T_c by 0.52 ± 0.05 K (such a difference is the signature of uniaxial anisotropy). Another estimate of the anisotropy scale was obtained by defining a reduced-temperature scale for the anisotropy: $\chi_b^{-1}(T_c)=\chi_c^{-1}(T_c+\Delta T_{\rm anis})$, where χ_c is the c-axis susceptibility. This procedure gave $\Delta T_{\rm anis}=0.57\pm0.09$ K.

Quasielastic neutron scattering on a ^{160}Gd-enriched single crystal[31] indicated the presence of anisotropic short-range order above and below T_c.

Recently a general method for the evaluation of lattice sums determining the effective parameters in the Hamiltonian of a dipolar magnetic system has been introduced.[32,33] This method was used to examine the anisotropy of the Hamiltonian as a function of c/a for a variety of lattices and it was found that dipole-dipole interactions favor the c axis as easy axis of magnetization for $c/a=1.59$, i.e., the c/a ratio for Gd at T_c. It was concluded[32,33] that the dipole-dipole interactions would themselves be sufficient, in the absence of any other interactions, to cause the observed uniaxial ordering at the Curie point. They estimated the temperature range for the uniaxial anisotropy to be $\Delta T_{\rm anis}\approx0.45$ K.

Fujiki, De'Bell, and Geldart[32] and Fujiki[33] proposed a sequence of overlapping crossovers to explain the observed critical behavior of Gd. According to their theory, relatively far away from T_c ($t>10^{-1}$) Gd is in the Gaussian regime, i.e., in the regime described by Landau theory with weak perturbations. When the reduced temperature is decreased, the Gaussian behavior is replaced first by the isotropic Heisenberg behavior and below $t\approx2.15\times10^{-2}$, by the isotropic dipolar regime. The crossover reduced temperature to the asymptotic critical

regime is $t \approx 1.52 \times 10^{-3}$ and the asymptotic critical regime is of uniaxial (Ising) type with dipolar interactions playing an important role.

The effect of the dipolar interactions on the critical behavior of Gd was also considered by Aliev, Kamilov, and Omarov[34] in their analysis of experimental results of magnetization and susceptibility measurements on two single crystals of Gd. Assuming that in the temperature range of the fits ($10^{-3} < t < 5 \times 10^{-2}$) the critical behavior of Gd is essentially governed by the isotropic dipolar forces they obtained good agreement between the calculated and fitted values of the correction to scaling terms.

Recent muon spin-relaxation time measurements on a spherical single crystal of Gd showed[35] a strong effect of a crossover from a nonconserved dynamics (dipolar) regime to a conserved (exchange dominated) regime $\sim$ 10 K above T_c and anisotropy in the muon relaxation rate along the c axis and in the basal plane for $t < 0.01$.

In summary, there is considerable experimental and numerical evidence that the critical behavior of Gd can be understood in terms of magnetic dipole-dipole interactions, and dipolar effects appear to be present throughout the range of virtually all experimental measurements of critical exponents of gadolinium.

Finally, it should be noted that logarithmic corrections characteristic of three-dimensional uniaxial dipolar magnets have not yet been conclusively observed experimentally in Gd. It is not trivial to detect multiplicative logarithmic corrections to the power laws even if the additional problems of crossover from Heisenberg behavior are not present. For instance, the magnetic susceptibility in the asymptotic uniaxial dipolar regime varies as $\chi \propto |t|^{-1} |\ln|t||^{1/3}$ and is dominated by strong $|t|^{-1}$ dependence (measurements over a few decades of reduced temperature may be needed to detect the slowly varying logarithmic term).[27] However, for heat capacity the logarithmic term, $|\ln|t||^{1/3}$, is the leading singular term,[28] and it is not masked by a power law. For that reason, high-resolution heat-capacity measurements on Gd, in the reduced-temperature range $|t| < 10^{-3}$, could provide further experimental evidence needed to determine the critical behavior of Gd.

III. EXPERIMENTAL METHOD

A complete description of the theory, design, and testing of the ac calorimeter used in this work has been given elsewhere,[36,37] and only the essential features are summarized here. Data tables with experimental heat capacities of Gd for all samples are available in Ref. 36.

The sample heat capacity in an ac experiment is given by

$$C \approx \frac{P}{\omega \Delta T} , \tag{1}$$

where P is the amplitude of the heating signal, ω is the frequency of the sample temperature oscillations, and ΔT is the amplitude of the temperature oscillations. The temperature probe senses the average ac temperature oscillations within the radius of the thermal diffusion length, the amplitude of which is determined by the local heating power and the heat capacity of the sample per unit of the sample surface area. Knowing the power density and the sample surface area one can calculate the total absolute heat capacity value from Eq. (1). However, because of the uncertainties involved in accurately determining the power dissipated in the sample, the sample surface area and the heater surface area, and inhomogeneities in the heater coverage, this procedure can give only a rough estimate of the absolute heat capacity of the sample. In our experiment, the data obtained by ac calorimetry were calibrated using the absolute heat-capacity data obtained by the relaxation-time method.[36,37]

The measurements on two single crystals of Gd (sample I and sample II) are reported here. Sample I was cut from an electrotransport-purified single crystal of Gd grown at the Ames Laboratory, Energy and Mineral Resources Institute. This crystal had been characterized by previous electrical resistance[9] [RR$=R(293\ \text{K})/R(4.2\ \text{K}) \approx 150$] and magnetic-susceptibility[15] studies. Sample I was cut from this crystal with a diamond saw. After cutting, sample I was around 0.32 mm thick and it was subsequently polished with No. 600 SiC paper and diamond paste (final polishing was done with 1 μm diamond paste). It was polished only to the extent needed to smooth out the rough surfaces left after cutting (final dimensions $5.34 \times 3.02 \times 0.32$ mm^3).

Sample I was subjected to three heat treatments. During the first heat treatment, it was cleaned in toluene and in acetone and heated from room temperature to 850 °C in a few minutes, annealed at 850 °C for 1 h and then cooled to room temperature over a few minutes (sample I after the first heat treatment is denoted sample I-1). All these thermal treatments took place in a continuous flow of high-purity helium (purity 99.999%). The sample was wrapped in tantalum foil, which acted as an oxygen trap.

During the second heat treatment sample I-1 was heated at 300 K/h from room temperature to 850 °C, held at 850 °C for 2 h and then cooled to room temperature over 24 h, all in flowing high-purity He. (Sample I after the second heat treatment is denoted sample I-2.)

In the third heat treatment the procedure from the second heat treatment was repeated but the sample was kept at 850 °C for 8 h (sample I-3).

Sample II was grown at the Ames Laboratory, Energy and Mineral Resources Institute, by recrystallization (grain-growth method) from a high-purity stock material produced by a metallothermic method.[47] The sample II purity was 99.89 at. % (99.99 mass%); the main impurities were oxygen, hydrogen, nitrogen, carbon, fluorine, and iron. (Chemical analysis for sample II is given in the Appendix.) The crystal from which sample II was made was grown to specified lateral dimensions and thickness of the order of 1 mm. This crystal was cut with a diamond saw into two pieces, each of thickness of the order of a fraction of a mm. The piece which had been glued to the backing during the cutting was electropolished and used for the measurements reported here as sample II (dimensions $7.4 \times 4.2 \times 0.22$ mm^3). The sample residual resistance ratio (RR) was not measured in order to avoid damage to the sample surface and also to avoid effects

due to thermal cycling of the sample. However, a Gd sample prepared in the same way and by the same laboratory was reported to have RR of the order of 200.[22]

IV. RESULTS

The heat capacity of sample I before annealing and after three consecutive heat treatments is shown in Fig. 1. The data points were collected every 100 mK; the temperature drift rate was 12 mK/min.

The first heat treatment induced a large smearing of the phase transition, considerable reduction of the peak value of the heat capacity, and a decrease in the critical temperature as estimated by the peak temperature, by around 2.5 K, in comparison with the unannealed sample (Fig. 1, curve I-1).

The heat-capacity curve determined after the second annealing is given by curve I-2 in Fig. 1. This heat treatment almost restored the peak temperature observed for the unannealed sample but the peak value of the heat capacity remained depressed.

The heat capacity of the sample after the third annealing is given by curve I-3 in Fig. 1. Curve I-3 nearly overlaps with curve I-2, however, curve I-3 is steeper on the high-temperature side of the transition than curve I-2.

The measured heat capacity of sample II is shown in Fig. 2. The data points shown in Fig. 2 were collected every 50 mK (temperature drift rate ~ 12 mK/min). Sample II exhibits the sharpest phase transition with the largest peak value of the heat capacity and the highest peak temperature of all samples investigated in this work.

In order to determine how the temperature drift rate affects the shape of the heat-capacity curve near T_c a series of measurements was carried out with temperature drift rates in the range from 3 mK/min to 72 mK/min.

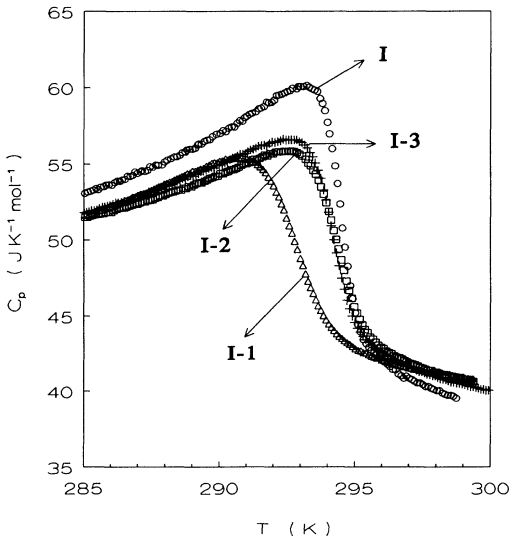

FIG. 1. The heat capacity of Gd near its ferromagnetic phase transition for sample I; curve I—heat capacity of unannealed sample; curves I-1, I-2, and I-3—heat capacity after consecutive heat treatments as described in the text.

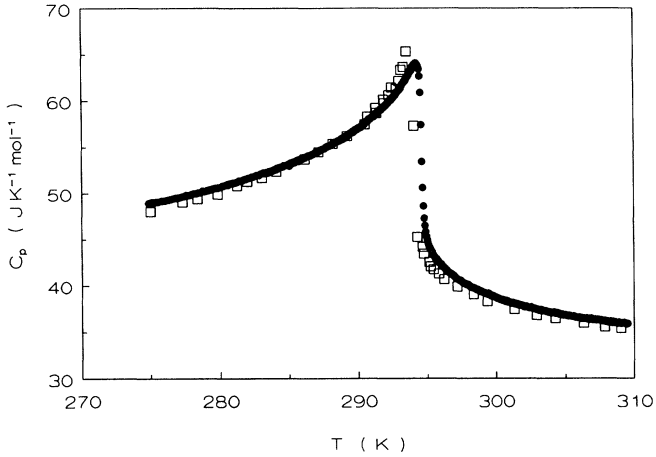

FIG. 2. ●, the measured heat capacity of Gd near its ferromagnetic phase transition for sample II; □, the heat-capacity data of Lanchester *et al.* (Ref. 20).

The results were not affected by these drift rate changes.

Heat capacities calculated from quantum-statistical models of phase transitions usually refer to constant geometry conditions, i.e., they assume fixed and temperature-independent unit-cell dimensions, angles and all atomic position parameters. Heat capacity at constant volume or, more generally, heat capacity at constant strain is a good approximation to the theoretical heat capacity provided that the sample volume does not change much in the temperature interval of measurements. The difference between the heat capacity at constant pressure and at constant strain, which for simplicity we refer to as ΔC_{p-V}, for a hexagonal crystal is quadratic in the diagonal components of the thermal-expansion tensor[38]

$$\Delta C_{p-V} = C_p - C_\epsilon = VT[2(c_{11}+c_{12})\alpha_a^2 + 4c_{13}\alpha_a\alpha_c + c_{33}\alpha_c^2] , \quad (2)$$

where the Voigt notation is used. This difference can be quite large if these components become divergent close to T_c.

Using the literature values of the elastic constants of Gd (Refs. 39 and 40) and the power-law representation of temperature dependence of α_a and α_c given by Dolejsi and Swenson,[22] ΔC_{p-V} was calculated from Eq. (2) for Gd in the temperature range from 285 to 300 K; the results are shown in Fig. 3. The average values of the elastic constants were taken over the short temperature range of the calculations. The critical temperature was assumed to lie within the rounded portion of the heat-capacity curve for sample II ($T_c = 294.5$ K in Fig. 3). As can be seen in Fig. 3 the difference between the heat capacity at constant pressure and at constant volume, ΔC_{p-V}, becomes important close to T_c, as this is the temperature range in which the thermal expansivities diverge rapidly. ΔC_{p-V} accounts for around 5% of the total heat capacity in the proximity of T_c for $T < T_c$. ΔC_{p-V} and measured C_p values were used to calculate heat capacity at

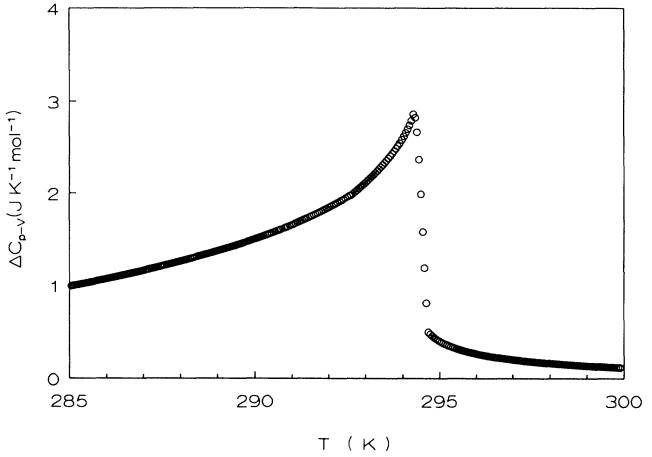

FIG. 3. The difference between the heat capacity of Gd at constant pressure and constant volume near the Curie temperature, calculated as described in the text.

TABLE I. The experimental heat capacities of Gd obtained by the relaxation method, in order of determination.

T (K)	C_p (J K^{-1} mol^{-1})
	Sample I
285.0	52.14
298.0	40.70
	Sample I-1
285.0	51.10
298.0	41.71
	Sample I-2
285.0	51.43
298.0	41.31
	Sample I-3
285.0	51.69
298.0	41.09
	Sample II
277.0	50.51
307.0	35.68

constant volume as a function of the reduced temperature in the proximity of T_c, shown in Fig. 4 (C_p data points for this graph were collected every 20 mK at a temperature drift rate of 12 mK/min).

The molar volume of Gd as a function of temperature near T_c also was calculated from the thermal-expansion data.[22] It decreases by around 0.2% in the temperature range 285–300 K so that in the temperature range of the critical point analysis, i.e., within a few K of T_c, the calculated heat capacity at constant and *temperature-dependent* volume approximates well the heat capacity at constant *geometry* required by the theory.

Heat-capacity values collected in the relaxation-time mode and used to calibrate the data obtained in the ac mode are listed in Table I. The precision of the relaxation time measurement, as estimated from standard deviations of the fits to the temperature decay data and to the thermal-conductance data, was around 2%. The data in the table are corrected for the heat capacity of the addenda using the literature data for the heat capacity of silver-loaded epoxy[41] and copper.[42] The correction terms contributed only a few percent to the total heat capacity of the sample assembly for samples I and II. The data were not corrected for the heat capacities of the General Electric varnish, bismuth layer, and the thinistor, since their combined mass (and combined heat capacity) was less than 2% of the total sample assembly.

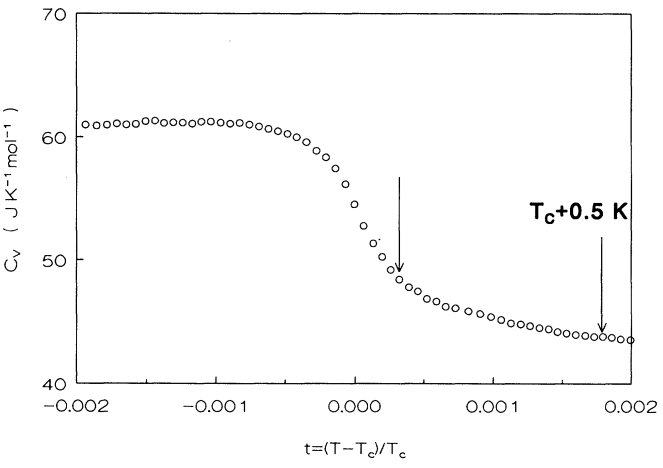

FIG. 4. The heat capacity of Gd in the proximity of the critical temperature as a function of the reduced temperature (data for sample II). Arrows indicate the temperature range of the logarithmic fit.

V. DATA ANALYSIS

A. Shape of the heat-capacity curve near T_c

To the best of our knowledge, this is the first report of high-resolution data on heat capacity of Gd, measured by the ac method and calibrated with absolute heat-capacity measurements made on the same sample. Lewis[17] reported his results in relative units and Simons and Salamon[19] calibrated their data using the data of Griffel, Skochdopole, and Spedding[43] near 0 °C. Wantenaar *et al.*[44] made ac heat-capacity measurements on relatively massive, cylindrical samples of Gd (approximate mass 3 g) and they calibrated their data with the use of Eq. (1). However this procedure led to differences in heat-capacity values for different samples as large as 20% far away from the phase transition (at temperatures of around 260 and 320 K). Wantenaar *et al.*[44] could not explain this deviation, which could have been caused by nonuniform heating of the samples.

High-resolution ac data on Gd were also reported by Simons and Salamon.[19] They do not report the resolution of their data. However, based on the information they give (temperature drift rate, heating frequency, and number of heating cycles averaged) the resolution of their data can be estimated to be around 50 mK. This resolution is comparable with the resolution of the present data. (We note however, that the resolution of the order

of a few mK is also possible with our calorimeter.[37]) The temperature scale of the Simons and Salamon[19] data was shifted in order to account for the different transition temperatures when making use of the data of Griffel, Skochdopole, and Spedding[43] for normalization. The peak value of the heat capacity of their data is around 62 J/mol K compared to our peak value of around 64 J/mol K and its temperature is around 1.5 K lower than the corresponding temperature for our data.

For comparison with the present data the absolute heat-capacity data of Lanchester *et al.*[20] (heat-capacity values taken from Fig. 1 of their paper) for a single crystal of Gd of quality comparable to the present samples are plotted in Fig. 2. The scatter of the data points obtained in this study, as estimated from the plot, is around 0.2%. There is good overall agreement between the data of this work and the data of Lanchester *et al.*[20] However, the temperature of the peak value of the heat capacity for the present data is around 0.6 K higher than the corresponding temperature for their data. Since in the data of Lanchester *et al.*[20] there is a temperature step of around 0.5 K between the peak value of the heat capacity and the next data point at increased temperature it is possible that a higher resolution in their measurements would reveal the maximum value of heat capacity to be at higher temperature. Higher resolution could also show rounding in their heat-capacity curve.

The differences between data on the heat capacity of Gd near the critical point reported by various authors are also likely caused by differences in sample quality. This view is supported by results of Robinson and Milstein[45] who investigated the influence of controlled amounts of carbon impurity on the shape of the heat capacity of Gd near the Curie point. Increasing the amount of carbon added from 0 to 1% decreased the magnitude of the heat-capacity peak and moved it towards lower temperatures.

Williams, Gopal, and Street[46] investigated the effects of strains on the heat capacity of polycrystalline samples of Gd near the Curie temperature. The sharpest phase transition and the highest peak value of the heat capacity with the highest peak temperature was obtained for the large-grained and annealed sample. The transition was depressed for the large-grained unannealed sample and significantly depressed and shifted to lower temperatures for the finely grained sample. Since all of the samples were of the same initial purity and zone melting does not result in significant purification of the sample (redistribution of impurities is the more usual result) Williams, Gopal, and Street[46] concluded that the broadening of the phase transition they observed was caused by different degrees of strains in the samples.

The conclusion of Williams, Gopal, and Street[46] is confirmed by the results of the heat-capacity measurements presented in this work. After the first heat treatment of sample I, considerable strain is expected to be frozen-in because of the fast cooling of the sample, producing a large amount of disorder. This disorder caused a marked broadening of the phase transition. The second and the third heat treatments almost restored the peak temperature to the value observed for the unannealed sample, but the peak value of the heat capacity remained depressed. The negligible improvement of the sharpness of the phase transition after the third heat treatment suggests that all the strains which were induced in the first heat treatment were removed. The remaining smearing was probably caused by sample contamination during one of the treatments. There also may have been dissolved gases such as oxygen, nitrogen, and hydrogen present in the initial crystal which could not be removed using the annealing procedures described here.[47] (One of the techniques used to purify rare-earth metals with respect to oxygen and nitrogen is electrotransport purification in ultrahigh vacuum.[47])

Gadolinium is known to absorb oxygen and hydrogen easily and it also oxidizes slowly when exposed to air.[47] The crystal from which sample I was cut had been exposed to air for long periods of time. This prolonged exposure to air may have a significant effect on the sample quality. For example Stetter, Farle, and Baberschke[16] measured the magnetic susceptibility of Gd films and found that exposing a Gd film to air reduced the peak in the susceptibility by a factor of 4. Williams, Gopal, and Street[46] observed that exposure to air of a polycrystalline sample of Gd contributed to the broadening of the heat-capacity curve at the critical temperature.

B. Analysis of the critical behavior

1. *Functions*

The analysis presented here focuses on the heat-capacity measurement of sample II of Gd, as this sample exhibited the sharpest transition and gave the highest value of the peak heat capacity of the measured samples.

The measured heat capacity at constant pressure, C_p, and the calculated heat capacity at constant volume, C_V, for sample II were each analyzed in terms of the fitting function

$$C_{p,V}=\frac{A}{\alpha}|t|^{-\alpha}(1+D|t|^{x})+B+Et \ , \tag{3}$$

for $T>T_c$ and the same functions with primed coefficients for $T<T_c$. The term $(A/\alpha)|t|^{-\alpha}$ represents the leading contribution to the singularity in C_p or C_V. If one assumes that $x>0$ then the term $D|t|^{x}$ vanishes at T_c and represents a singular contribution to the heat capacity which is of higher order than the leading singularity. It is known both from experiments[48] and theory[49,50] that such a term generally must be considered in the data analysis ($x=x'=0.5$ in the present analysis).

The data in the proximity of T_c also were fitted to the function

$$C=A|\ln|t/t_0||^{1/3}+B \ , \tag{4}$$

for $T>T_c$ and the same function with primed coefficients for $T<T_c$. The values of the ratios $A/A'=1/4$ and $t_0/t_0'=2$ were constrained to those predicted by the theory.[27,51]

It is difficult to interpret data extremely near T_c in terms of Eqs. (3) and (4) because of rounding in the heat-

capacity curve in that region. Certainly, the data affected by rounding should not be fit to Eq. (3) or Eq. (4) without some modifications, which depend on possible causes of rounding. These rounded data were excluded from the analysis in terms of the fitting functions given in this section. The factors which may contribute to the rounding were discussed in Sec. V A and will be summarized in the last section of this paper.

The fitting procedure employed here allows simultaneous fitting of both linear and nonlinear contributions to the heat capacity. The computer program used performs a nonlinear least-squares fit to data. The program was initially developed by Malmström and Geldart[52] and subsequently extended. It has been used previously to analyze resistivity[9] and magnetic-susceptibility data[15] on Gd and heat-capacity data on Ni.[52]

2. *Fitting procedure*

It was assumed initially that $D=D'=0$. The seven parameters (A, A', $B=B'$, $T_c=T_c'$, α, α', and $E=E'$) were least-squares adjusted. (The condition $E=E'$ was imposed to assure that the regular contribution to the total heat capacity is indeed regular at T_c.) The data were analyzed in the temperature range $t_{\min}<|t|<t_{\max}$, where $t_{\min}$ and $t_{\max}$ are defined with respect to the initial choice for T_c.

In the first step of the analysis A, A', $B=B'$, and $\alpha=\alpha'$, were fitted for a fixed value of T_c in the temperature range in which data affected by rounding were excluded. If the fitting routine converged, the next step was to allow T_c also to be fitted. If T_c could be fitted, the statistical parameters of the fit [the estimated standard deviation of the fit, the estimated 95% confidence intervals in the fitted parameters, the plot of residues (the difference between the measured C and the fit to the data) and the histogram of the residues] were printed out and analyzed. At the beginning almost all the data were kept in the fitted data set, and the plot of residues showed the presence of systematic structures near T_c in the region of the heat-capacity curve affected by rounding. This indicated the poor quality of the fit and unreliable representation of the data. Removing the data points affected by rounding resulted in a significant improvement of the fit quality.

Alternatively, the best fit was located by least-squares fitting A, A', $B=B'$, and $E=E'$ for T_c and α stepped over a range of values; this best fit was then compared with the fit obtained by least-squares fitting of all the parameters in order to select the fit giving the smallest standard deviations and the best plot of residues. In practice these two procedures gave the same result, serving as a consistency check.

In the next step a range of fit analysis was performed for different values of $t_{\max}$ and $t_{\min}$. In this analysis the data were fitted for decreasing values of $t_{\max}$. This was done in order to find the temperature range in which α was not sensitive to further decrease in $t_{\max}$. In a similar way $t_{\min}$ was increased to see if this was going to bring about a further improvement in the fit quality. While the reason for varying $t_{\max}$ is to find the beginning of the asymptotic critical region, one generally insists that $t_{\min}$ be kept as close to T_c as possible.[53] However, in the case of Gd the presence of crossovers also justifies seeking the temperature range in which a given fitting function best represents the data.

After finding the best $t_{\min}$ and $t_{\max}$ two predictions of the renormalization-group theory were tested. First, α was permitted to be different from α'. In each case, α and α' overlapped within the standard errors and thus permitted $\alpha=\alpha'$, consistent with the scaling prediction. Secondly, the constraint $B=B'$ was tested. It was found that in the limited temperature range in which the pure power law gave a good fit, $B=B'$ within experimental error.

The data also were analyzed in the same way by fitting to Eq. (3) with D and D' least-squares adjusted. The constraints $\alpha=\alpha'$, $E=E'$, and $B=B'$ were retained and $x=x'$ was fixed at 0.5, consistent with the theoretical predictions and other experiments.[54]

Finally, the data for sample II very close to T_c were fitted to Eq. (4). The parameters in Eq. (4) were fitted for different fixed values of T_c. The constraints on each parameter were systematically relaxed to test whether this was going to improve the fit. This fitting was performed for the combined data from the both sides of the transition, and also for the high-temperature side of the transition separately.

3. *Results*

The parameters obtained by fitting the heat-capacity data for sample II to Eq. (3) are given in Table II.

The analysis for sample II started by finding the best pure power-law fit and the correction to scaling fit to the C_p data. It was found that generally a reasonable power-law fit was possible over a rather wide temperature range (the range overlapped with the temperature range of the correction to scaling fit given in Table II). However, a subsequent range-of-fit analysis showed that the quality of the fit could be improved considerably by decreasing $t_{\max}$. It also was found that the fit could be improved by dropping a number of points close to T_c, i.e., by increasing $t_{\min}$, although the excluded points did not appear affected by rounding. Thus, the best power-law fit was obtained over a rather restricted reduced-temperature range, which however, lay in the critical region. Both T_c and α were least-squares fitted in this analysis.

Inclusion of the confluent correction to scaling term in the fit brought about a decrease in the standard deviation of the fit and also permitted a good fit in a wider temperature range (over one decade in the reduced temperature).

The exponent α and the critical temperature were determined by fitting A, A', D, D', $B=B'$, and $E=E'$ for a range of T_c and α values.

The C_V data for sample II were fitted separately to Eq. (3); the results also are given in Table II.

Finally the C_V data for sample II in the proximity of T_c ($t<10^{-4}$) were fitted to Eq. (4). Both sides of the transition were used in the fit and the constraints $A/A'=1/4$ and $t_0/t_0'=2$ were initially imposed.[27,51] When a good fit could not be obtained these constraints were either relaxed or the ratios changed to other values.

However a satisfactory fit was not obtained.

As discussed in the next section, the low-temperature side of the transition could be affected by an unknown temperature dependence of the demagnetization energy which may be important close to and below T_c. Because of that the high-temperature side of the transition was fitted separately to Eq. (3) and Eq. (4).

A good logarithmic fit was obtained over the 10^{-4} decade in the reduced temperature ($3.2\times10^{-4}<t<1.7\times10^{-3}$) for $T_c=294.6$ K (the fit range is indicated by arrows in Fig. 4; the estimated standard deviation of the fit $\sigma_{\rm FIT}=0.0855$). The fit was based on 20 data points. The other parameters of the fit were $B=-11.5\pm1.6$, $A=29.8\pm0.8$, with the constraint $t_0=1$. Other values of t_0 were tested and $\sigma_{\rm FIT}$ was minimized for $t_0=1$.

The power-law fit in the same range gave the least-squares adjusted $\alpha=0.98\pm0.07$. This is a physically unrealistic result and is discussed later.

In order to obtain a good power-law fit to the heat-capacity data for the remaining samples a large number of points affected by rounding had to be excluded in each case from the fit. This resulted in removing almost all data points below $t=5\times10^{-3}$ from the analysis. Because of the strong sample dependence of the fits and the large gaps around T_c, we do not consider those fits to give meaningful information about the critical behavior of Gd and we do not analyze them here.

TABLE II. Results of fitting the data for sample II. The estimated errors are 95% confidence intervals obtained from the fits assuming independent and random errors in the heat capacity measured.

	PL-C_p[a]	CRSC-C_p[b]	PL-C_V[c]	CRSCI-C_V[d]	CRSCII-C_V[e]
T_c	294.25 ±0.05	294.5[f] ±0.05	294.2 ±0.1	294.5[f] ±0.1	294.5[f] ±0.1
α	−0.208 ±0.014	−0.026[f] ±0.002	−0.187 ±0.023	−0.020[f] ±0.002	−0.020[f] ±0.002
A'	1.57 ±0.34	1.14 ±0.20	2.07 ±0.28	0.60 ±0.41	0.75 ±0.20
A	16.1 ±2.1	1.74 ±0.20	11.7 ±4.8	0.98 ±0.40	1.13 ±0.20
A/A'	10.3 ±2.6	1.53 ±0.32	5.65 ±2.44	1.63 ±1.29	1.51 ±0.48
D'		1.15 ±0.36		1.17 ±0.49	1.00 ±0.36
D		0.58 ±0.15		1.36 ±0.68	0.98 ±0.27
D/D'		0.51 ±0.21		1.17 ±0.77	0.98 ±0.46
E	508 ±54	63 ±30	295 ±50	148 ±85	105 ±35
B	65.8 ±0.7	102 ±6	64.3 ±2.7	89 ±17	95 ±9
$\sigma_{\rm FIT}$	0.0604 ±0.0091	0.0545 ±0.0060	0.0641 ±0.0089	0.0580 ±0.0081	0.0574 ±0.0067

[a]PL-C_p: power-law fit to C_p data. Range of the fit: $t=5.9\times10^{-3}$–0.5×10^{-3}, $T<T_c$; $t=3\times10^{-3}$–6.9×10^{-3}, $T>T_c$. 75 data points in the fit.

[b]CRSC-C_p: fit with the correction to scaling term to C_p data. Range of the fit: $t=15.3\times10^{-3}$–2.6×10^{-3}, $T<T_c$; $t=2.0\times10^{-3}$–11.9×10^{-3}, $T>T_c$. 130 data points in the fit.

[c]PL-C_V: power-law fit to C_V data. Range of the fit: $t=9\times10^{-3}$–0.7×10^{-3}, $T<T_c$; $t=3\times10^{-3}$–8×10^{-3}, $T>T_c$. 79 data points in the fit.

[d]CRSCI-C_V: correction to scaling fit to C_V data over the temperature range of the power-law fit.

[e]CRSCII-C_V: fit with the correction to scaling term to C_V data. Range of the fit: $t=12\times10^{-3}$–1.7×10^{-3}, $T<T_c$; $t=1.7\times10^{-3}$–13×10^{-3}, $T>T_c$. 116 data points in the fit.

[f]As described in the text, in the case of fits including correction to scaling, T_c and α were varied with fixed increments over a range of values, while the other parameters were least-squares adjusted. Error limits in T_c and α indicate the increments below which $\sigma_{\rm FIT}$ showed negligible variations.

VI. DISCUSSION

A. Critical exponent α

Measurements of heat capacity over magnetic phase transitions in solids show rounding of the heat-capacity curve in the proximity of T_c, even though model systems have singularities, such as cusps, at T_c. The rounding of the heat-capacity curve is present even in measurements on very high-quality crystals and it affects the heat-capacity data in the 10^{-5} decade and also most of the data in the 10^{-4} decade in reduced temperature.[55–57] The data affected by rounding are discarded in fitting so that the results are usually based on the 10^{-3} decade in the reduced temperature. The values of fitted parameters are effective values reflecting fitting in a preasymptotic region and possible crossovers.

In contrast with magnetic phase transitions in solids, phase transitions in liquid crystals are much sharper and in some cases high-resolution heat-capacity data over almost three decades in reduced temperature (from $t=10^{-3}$ to $t\approx10^{-5}$) can be used for fitting, making it possible to fit the first as well as the second correction to scaling term.[58]

As can be seen in Table II the best representation of both C_p and C_V data for sample II was obtained in terms of the correction to scaling fit. This fit gave the smallest standard deviation and represented the data over the widest temperature range (Fig. 5). The pure power-law fit to C_p and C_V data gave a standard deviation similar to that for the fits with the correction to scaling term but it represented the data over a narrower temperature range and it also gave unphysically large values of the ratio A/A' and of the regular term E. The exponent α from the pure power-law fits agrees with the value $\alpha=-0.20\pm0.02$ obtained by Simons and Salamon[19] also from the analysis with a power law.

The values of the fitted parameters given in Table II for the fits with the correction to scaling term are in good agreement with the corresponding results obtained by Jayasuriya[21] who remeasured the heat capacity of the Gd crystal used by Lanchester *et al.*[20] and obtained a good fit to the data with the constraint $\alpha=\alpha'$ after including the confluent singular term into the fit. Jayasuriya obtained $\alpha=-0.03\pm0.02$ and the universal ratios

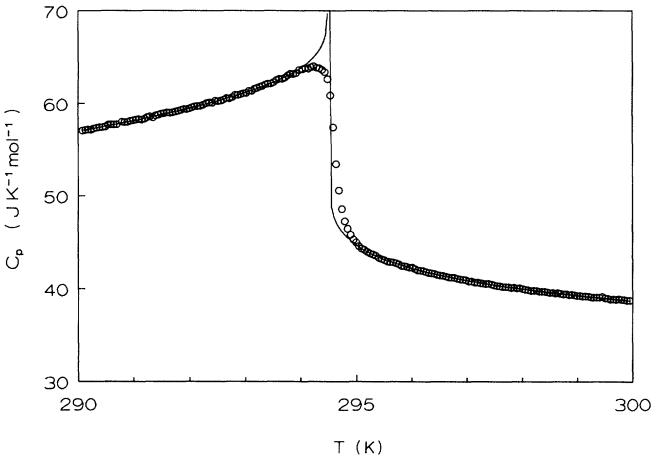

FIG. 5. Fit of Eq. (3) with the correction to scaling term (——) to the C_p data (○) for sample II.

$A/A'=1.42\pm0.75$ and $D/D'=0.71\pm0.56$, and also $B=108\pm12$. Jayasuriya[21] and Lanchester *et al.*[20] reported that a good pure power-law fit to their data over a wide temperature range also was obtained when a discontinuity in the heat capacity at T_c was allowed ($B\neq B'$). It appears that if such extra free parameters are needed to fit the data one should instead introduce the confluent singular correction term predicted by the renormalization-group theory.

The correction to scaling fit to the C_V data for sample II gave values of the parameters of the fit that were different from those for the same fit to the C_p data. The ratio A/A' did not change within the statistical error but the magnitude of the exponent α became smaller and the ratio D/D' increased. The heat capacities at constant volume were calculated using the thermal-expansion and elastic constant data close to T_c measured on different Gd samples. Since those data are likely to be sample dependent (at least in the proximity of T_c) it is difficult to say if the differences in the values of α and of the D/D' ratio reported here should be regarded as significant. However they suggest that the reduction of the experimental data collected at constant pressure to the heat-capacity data at constant volume may be an important consideration for Gd, and it may also be relevant in other materials.

The RG calculations[59,60] give $(A/A')_H=1.52\pm0.02$ in three dimensions for the Heisenberg universality class in the second-order ϵ expansion. The ratio $(A/A')_{\rm dip}$ for a system with both isotropic short-range and dipolar interactions is known only to the zeroth order in ϵ: The ratio is $1.2+O(\epsilon)$. $A/A'=1$ to the zeroth order for the Heisenberg (short-range) 3d system suggests that $(A/A')_{\rm dip}>(A/A')_H$ although the difference is not expected to be large.[60]

The ratio $D/D'=1.4$ for the Heisenberg system in three dimensions, as given by the field-theoretical methods.[59]

The ratios $A/A'=1.51\pm0.48$ and $D/D'=0.98\pm0.46$ obtained for the C_V data here are in reasonable agreement with the ratios for the Heisenberg system; if, as suggested by other evidence, in the temperature range of the fit Gd is in the process of crossing over to dipolar isotropic behavior from the Heisenberg behavior then these ratios are certainly plausible.

The critical exponent $\alpha=-0.020\pm0.002$, as determined from the correction to scaling fit to the C_V data should be regarded as an effective exponent. This view can be supported by noting that the scaling laws for effective exponents are correct to the zeroth order in the ϵ expansion[61,62] so that, for example, $\alpha_{\rm eff}\approx2-2\beta_{\rm eff}-\gamma_{\rm eff}$. This relation and the experimentally determined values of $\gamma\approx1.22\pm0.02$ for $t>10^{-3}$, as measured on a sample cut from the crystal used to obtain sample I in this work[15] and $\beta\approx0.399\pm0.016$ (the most recent value of β obtained by Chowdhury, Collins, and Hohenemser[4] from $\gamma\gamma$ angular-correlation experiment and the fit with the correction to scaling term to their data for $t>10^{-3}$) give $\alpha_{\rm eff}\approx-0.02\pm0.03$, in good agreement with the experimental value obtained here. This value for $\alpha_{\rm eff}$ is also consistent with experimental results for the temperature dependence of the susceptibility of Gd in the hard direction, χ_b, reported by Geldart *et al.*[10] χ_b^{-1} is expected to vary with t as $A+Bt^y$, $y=1-\alpha_{\rm eff}$ and their fit to $\chi_b^{-1}(T)$ data yielded $y=1.01\pm0.03$. A correction to scaling term was not used in their analysis. Their corresponding $\alpha_{\rm eff}\approx2-2\beta_{\rm eff}-\gamma_{\rm eff}$ determined with no correction to scaling terms was[10] $\alpha_{\rm eff}=-0.05\pm0.04$.

It should be noted that the effective exponent α for a crossover from the Heisenberg to the isotropic dipolar behavior need not be expected to take an intermediate value between the value of α for the Heisenberg system ($\alpha\approx-0.125$) and the value of α for the isotropic dipolar system ($\alpha\approx-0.135$). Using renormalization-group methods to the leading order in $\epsilon=4-d$, Bruce, Kosterlitz, and Nelson[63] showed that for $-2<\log\tilde{t}<2$, where $\tilde{t}=t/\hat{g}$ and $\hat{g}$ is a dimensionless parameter measuring the strength of dipolar interactions, the effective exponent α for a crossover from the Heisenberg to the isotropic dipolar behavior varies strongly as a function of $\tilde{t}$ (their fits covered one decade on each side of a given $\tilde{t}$) taking values from around -0.1 to 0.1. For Gd, $\hat{g}\approx5\times10^{-3}$, as estimated by Geldart *et al.*[10] and taking $t_M\approx5\times10^{-3}$, where t_M is the middle of the fit range for the correction to scaling fits one obtains $\log\tilde{t}\approx0$. Thus, our α is obtained from the fit in the reduced temperature range where the exponent α is expected to be strongly affected by crossover effects.

B. Universal ratio R_{Bc}

Bagnuls and Bervillier[64] introduced the universal ratio, R_{Bc}, involving the critical contribution B_c to the background term B in the expression for the critical heat capacity:

$$R_{Bc}=A|D|^{\alpha/\Delta}(\alpha B_c)^{-1}\ . \tag{5}$$

The critical contribution B_c is defined by $B_c=B-B_r$. The regular term B_r equals B far away from criticality. We estimated B_r in two ways: using the high-

temperature Gd heat capacity of Jayasuriya,[21] $B_r = 31 \pm 1$ J mol^{-1} K^{-1}; from the heat capacity of the nonmagnetic rare-earth metal lutetium,[65] $B_r = 26.8 \pm 0.5$ J mol^{-1} K^{-1}. Using the fitted value of B from the correction to scaling fit to C_V data we obtained $R_{Bc} = -0.88 \pm 0.34$ and $R_{Bc} = -0.83 \pm 0.33$, respectively. Theoretically calculated values of R_{Bc} for various spin dimensionalities, n, in three dimensions are[66] $-0.7081(5)$ for $n=1$, $-1.057(22)$ for $n=2$, and $-1.3785(41)$ for $n=3$. The values of R_{Bc} obtained here appear to be inconsistent with the value for the Heisenberg system but they add further support for the view that Gd becomes uniaxial close to T_c.

It has to be noted, however, that conclusions based on the experimentally found value of R_{Bc} may be illusory. Careful examination of Eq. (5) shows that the ratio R_{Bc} is around unity for values of α not much different from zero with little sensitivity to the values of the other parameters. (This feature of this ratio was first noticed by Singsaas and Ahlers.[67]) This can be seen by writing Eq. (5) in terms of the function

$$C_p = \frac{A}{\alpha}[(|t|^{-\alpha}-1)+D|t|^{x}]+B_c'+B_r+Et \ , \tag{6}$$

where $B_c' = B_c + A/\alpha$. The ratio R_{Bc} is now

$$R_{Bc} = \frac{-|D|^{\alpha/\Delta}}{1-\alpha B_c'/A} \ . \tag{7}$$

The numerator in Eq. (7) will be very close to unity because α is very small. The ratio B_c'/A is also of the order of unity so it follows that roughly $R_{Bc} \approx -1+O(\alpha)$ which is close to unity for α close to zero. Thus a more stringent test may be to require good agreement between theoretical and experimental values for $R_{Bc}+1$.[67] At this level the agreement between our values and the theoretical value for $n=1$ appears less conclusive.

C. Uniaxial asymptotic critical regime

Finally we would like to turn to the discussion of a contribution from the demagnetization effects to the heat capacity of Gd near T_c. In the renormalization-group theory of magnetic systems with dipolar interactions the contribution to the free energy of the system from the demagnetization effects is neglected by assuming that the sample consists of one magnetic domain and that the bulk magnetization is uniform.[60] This requirement is satisfied for needle-shaped samples. (If an external magnetic field is present it has to be parallel to the long axis of the sample.) However, for samples of other shapes the free energy and hence the heat capacity will have a contribution from the demagnetization effects. Knowledge of the magnitude of such a correction term is particularly important close to T_c because of the possible effect of this correction on the critical behavior of the heat capacity.

We calculated the contribution of the demagnetization heat capacity to the total heat capacity near T_c for a rectangular slab of a ferromagnetic material in the mean-field approximation. The full account of this analysis is given elsewhere.[68] For Gd samples used in this work the results of this analysis suggest that the contributions from demagnetization effects to the heat capacities are negligible over almost the entire experimentally accessible temperature range, even with a high-resolution heat-capacity measurement. However, it was also noted[68] that if there are significant data available below $t = 10^{-4}$ for $T < T_c$ then the contribution from the demagnetization effects may make it impossible to fit the data points in this temperature range with currently available expressions pertinent to the critical behavior of Gd.

In order to take that possibility into account the data on the high-temperature side of the transition were fitted separately to Eq. (3) and Eq. (4). As reported in the preceding section a good fit to the data of the logarithmic form given by Eq. (4) was obtained in the 10^{-4} decade of the reduced temperature for $T > T_c$. The range-of-fit analysis for the temperature intervals starting between $t_{\min}$ and $t_{\max}$ and extending above $t_{\max}$ showed that Eq. (4) gave a good representation of the data only very close to T_c. A power-law fit performed in the temperature range of the logarithmic fit converged on the unphysical value $\alpha \approx 1$ thus indicating that another physical model should be used to describe the data in this temperature region.

The value of $t_{\max}$ is in good agreement with the estimate of the crossover reduced temperature to the asymptotic uniaxial regime, $t \approx 1.52 \times 10^{-3}$ ($\Delta T = T - T_c \approx 0.45$ K), given by Geldart *et al.*[10] This $t_{\max}$ is also in agreement with the experimental values of 0.52 ± 0.05 K and 0.57 ± 0.09 K obtained by Geldart *et al.*[10] from the magnetic-susceptibility measurements and the experimental value of $t \approx 1.3 \times 10^{-3}$ ($\Delta T = T - T_c \approx 0.38$ K) suggested by Dolejsi and Swenson[22] as a crossover temperature to a new critical regime on the basis of their fit to thermal-expansion data. These results appear to indicate that the critical behavior of Gd very close to T_c is that of the uniaxial system with dipolar interactions. Since it was not possible to fit the data very near T_c on both sides of the transition, the important theoretical amplitude ratio $A/A' = 1/4$ could not be tested.

Certainly one of the reasons for the failure of the logarithmic fit to both sides of the phase transition is the rounding in the heat-capacity curve over much of the temperature range where uniaxial dipolar behavior is expected. ΔT_{anis} is very small relative to T_c for Gd and this limits the reduced-temperature range available to an analysis with the logarithmic formula for this material.

It is known from experiments on Gd (Refs. 14, 45, and 46) and other magnetic systems (Ref. 69) that sample imperfections (impurities and dislocations) can lead to a large broadening of the phase transition and a decrease in the critical temperature. Sample II was very pure and it compared very well with other Gd samples measured. It is difficult to quantify, however, the importance of the dislocations (and hence strains) still present in the sample. The results presented here show how sensitive the phase transition in Gd is to the presence of strains. It is possible that in spite of its high purity and the care in preparation the rounding observed for sample II is caused by dislocations still present in the sample.

Another factor limiting the sharpness of the phase transition in Gd and changing the shape of the heat-capacity curve below T_c may be the demagnetization

effects and formation of magnetic domains. As noticed by Kadanoff *et al.*[70] the domain walls may serve to break up the long-range correlations so essential to critical behavior. Dislocations and other static defects can serve as the domain nucleation centers and pinning sites. The domain formation and the presence of an essentially random distribution of domain nucleation centers and pinning sites may lead to smearing of the transition.

VII. SUMMARY

In this paper we described the results of a high-resolution ac calorimetric investigation near a phase transition, Gd in the vicinity of its Curie point. These measurements showed that the calorimeter permits the measurement of very small samples (<20 mg) with temperature resolution of a few mK and sensitivity of around 0.2%.

The systematic investigation of the heat capacity of Gd near T_c for single crystals of Gd subjected to different heat treatments and preparation procedures showed that the presence of strains and associated dislocations in Gd leads to a broadening of the phase transition. It was suggested that, since dislocations are always present in real crystals, this may be an important reason for rounding of the phase transition observed even in crystals of very high purity.

It also was suggested that the formation of magnetic domains may affect the measured heat capacity very close to T_c and may also contribute to the observed rounding of the heat capacity near the peak temperature. The effect may be particularly pronounced in the presence of a random distribution of domain nucleation and pinning sites.

It also was found that the difference between the heat capacity at constant pressure and at constant volume for Gd is significant near T_c and should be taken into account in data analyses.

Analyses of the critical behavior of Gd were carried out in terms of power laws, power laws with the correction to scaling term, and the logarithmic expression characteristic of the critical behavior of uniaxial systems with dipolar interactions in three dimensions, i.e., at their critical dimension. The results of these analyses showed that the best representation of the data in the reduced temperature range from $t=10^{-2}$ to $t=10^{3}$ was obtained in terms of the power law with the correction to scaling term. The critical exponent, $\alpha=-0.020\pm0.002$, obtained from a correction to scaling fit to the C_V data was interpreted as an effective exponent; it was shown using the literature data for the critical exponents β and γ that the exponent α obtained from this experiment satisfied scaling relations for the effective exponents.

The values of the ratios A/A' and D/D' of the critical amplitudes and correction to the critical amplitudes, respectively, were found to be consistent with crossover from the Heisenberg critical regime to the isotropic dipolar regime in the temperature range of the fit.

The value of the universal ratio R_{Bc} obtained here supports the view that Gd becomes uniaxially ordered close to T_c.

Finally, since the data close to T_c on the low-temperature side of the transition may be affected by formation of domains which are not yet accounted for by the renormalization-group theory, the data on the high-temperature side of the transition were analyzed separately. A good fit to these data was obtained with the logarithmic law in the reduced temperature interval, $3.2\times10^{-4}<t<1.7\times10^{-3}$, determined by a range-of-fit analysis. A meaningful fit to the data in the same temperature range could not be obtained on the basis of power laws. The range of fit determined for the logarithmic behavior is in agreement with estimates of the temperature scale of the uniaxial anisotropy obtained from other experiments and numerical calculations.

ACKNOWLEDGMENTS

We are grateful to B. Millier, R. Conrad, D. Maclean, B. Fullerton, and R. Dunlap for technical assistance, and C. W. Garland for useful comments. This work was supported by the Natural Sciences and Engineering Research Council of Canada (grants to D. J. W. G. and M. A. W.) and the Killam Trust.

APPENDIX: CHEMICAL ANALYSIS FOR SAMPLE II

TABLE III. Spark surface mass spectrometric analysis in atomic ppm.

Li < 0.1	Be < 0.01	B < 0.09	Na < 0.2	Mg < 0.2
Al < 2	Si < 1	P < 0.1	S < 0.3	Cl < 2
K < 1	Ca < 1	Ti < 0.6	V < 2	Cr < 4
Mn < 0.06	Co < 0.1	Ni < 5	Cu < 6	Zn < 0.18
Ga < 0.2	As < 1	Se < 0.4	Br < 0.5	Rb < 0.06
Sr < 0.2	Zr < 0.6	Nb < 1	Mo < 1	Ru < 0.6
Rh < 0.1	Pd < 0.3	Ag < 0.05	Cd < 0.1	In < 0.06
Sn < 0.07	Te < 0.1	I < 0.06	Cs < 0.006	Ba < 0.1
Hf < 2	Ta < 12	Re < 0.8	Os < 1	Ir < 0.5
Pt < 0.7	Au < 0.1	Hg < 0.1	Tl < 0.09	Pb < 0.3
Bi < 0.07	Th < 0.9	U < 0.4		
		Rare-earth impurities		
Sc < 0.05	Y < 0.63	La < 0.5	Ce < 1	Pr < 0.5
Nd < 2	Sm < 2	Eu < 0.2	Tb < 3	Dy < 1
Ho < 0.4	Er < 1	Tm < 0.4	Yb < 4	Lu < 2

TABLE IV. Vacuum fusion results in atomic ppm.

O≈344	N≈45	H≈622	C≈131	F<25
Fe<18.5	W<0.86			

The analyses were provided by the sample producer.

*Author for correspondence.

[1]K. G. Wilson, Phys. Rev. B **4**, 3174 (1971); Rev. Mod. Phys. **47**, 773 (1975).
[2]A. R. Chowdhury, G. S. Collins, and C. Hohenemser, Phys. Rev. B **30**, 6277 (1984).
[3]D. H. Martin, *Magnetism in Solids* (London Iliffe Books, London, 1967).
[4]A. R. Chowdhury, G. S. Collins, and C. Hohenemser, Phys. Rev. B **33**, 6231 (1986).
[5]H. E. Nigh, S. Legvold, and F. H. Spedding, Phys. Rev. **132**, 1092 (1963).
[6]C. D. Graham, Jr., J. Appl. Phys. **36**, 1135 (1965).
[7]J. W. Cable and E. O. Wollan, Phys. Rev. **165**, 733 (1968).
[8]F. Milstein and L. B. Robinson, Phys. Rev. **177**, 904 (1969).
[9]D. J. W. Geldart, K. De'Bell, J. Cook, and M. J. Laubitz, Phys. Rev. B **35**, 8876 (1987).
[10]D. J. W. Geldart, P. Hargraves, N. M. Fujiki, and R. A. Dunlap, Phys. Rev. Lett. **62**, 2728 (1989).
[11]M. Vicentini-Missoni, R. I. Joshep, M. S. Green, and J. M. H. L. Sengers, Phys. Rev. B **1**, 2312 (1970).
[12]M. N. Deschizeaux and G. Develey, J. Phys. (Paris) **32**, 319 (1971).
[13]G. H. J. Wantenaar, S. J. Campbell, D. H. Chaplin, T. J. McKenna, and G. V. H. Wilson, J. Phys. C **13**, L863 (1980).
[14]G. H. J. Wantenaar, S. J. Campbell, D. H. Chaplin, T. J. McKenna, and G. V. H. Wilson, Phys. Rev. B **29**, 1419 (1984).
[15]P. Hargraves, R. A. Dunlap, D. J. W. Geldart, and S. P. Ritcey, Phys. Rev. B **38**, 2862 (1988).
[16]U. Stetter, M. Farle, and K. Baberschke, Phys. Rev. B **45**, 503 (1992).
[17]E. A. S. Lewis, Phys. Rev. B **1**, 4368 (1970).
[18]D. S. Simons, Ph. D. thesis, University of Illinois at Urbana-Champaign, 1973.
[19]D. S. Simons and M. B. Salamon, Phys. Rev. B **10**, 4680 (1974).
[20]P. C. Lanchester, K. Robinson, D. P. Baker, I. S. Williams, R. Street, and E. S. R. Gopal, J. Magn. Magn. Mater. **15-18**, 461 (1980).
[21]K. D. Jayasuriya, Ph.D. thesis, Australian National University, 1984.
[22]D. A. Dolejsi and C. A. Swenson, Phys. Rev. B **24**, 6326 (1981).
[23]J. C. LeGuillou and J. Zinn-Justin, Phys. Rev. B **21**, 3976 (1980).
[24]G. Ahlers, A. Kornblit, and H. J. Guggenheim, Phys. Rev. Lett. **34**, 1227 (1975).
[25]D. P. Landau, J. Phys. (Paris) Colloq. **32**, C1-1012 (1971).
[26]J. Kötzler and G. Eiselt, Phys. Lett. **58**, 69 (1976).
[27]A. I. Larkin and D. E. Khmelnitzkii, Zh. Eksp. Teor. Fiz. **56**, 2087 (1969) [Sov. Phys. JETP **29**, 1123 (1969)].
[28]A. Aharony and P. C. Hohenberg, Phys. Rev. B **13**, 3081 (1976).
[29]D. J. W. Geldart and T. G. Richard, Phys. Rev. B **12**, 5175 (1975).
[30]G. S. Collins, A. R. Chowdhury, and C. Hohenemser, Phys. Rev. B **33**, 4747 (1986).
[31]H. R. Child, Phys. Rev. B **18**, 1247 (1978).
[32]N. M. Fujiki, K. De'Bell, and D. J. W. Geldart, Phys. Rev. B **36**, 8512 (1987).
[33]N. M. Fujiki, Ph.D. thesis, Dalhousie University, Halifax, 1989.
[34]K. K. Aliev, I. K. Kamilov, and A. M. Omarov, Zh. Eksp. Teor. Fiz. **94**, 153 (1988) [Sov. Phys. JETP **67**, 2262 (1988)].
[35]E. B. Karlsson, Hyperfine Inter. **64**, 331 (1990).
[36]G. Bednarz, Ph.D. thesis, Dalhousie University, Halifax, 1992.
[37]G. Bednarz, B. Millier, and M. A. White, Rev. Sci. Instrum. **63**, 3944 (1992).
[38]J. F. Nye, *Physical Properties of Crystals* (Clarendon, Oxford, 1985).
[39]D. C. Jiles and S. B. Palmer, J. Phys. F **10**, 2857 (1980).
[40]E. S. Fisher, M. H. Manghnani, and R. Kikuta, J. Phys. Chem. Solids **34**, 687 (1973).
[41]A. Berton, J. Chaussy, J. Ocin, and B. Souletie, Cryogenics **17**, 584 (1977).
[42]R. Hultgren, R. L. Orr, P. D. Anderson, and K. K. Kelley, *Selected Values of Thermodynamic Properties of Metals and Alloys* (Wiley, New York, 1963).
[43]M. Griffel, R. E. Skochdopole, and F. H. Spedding, Phys. Rev. **93**, 657 (1954).
[44]G. H. J. Wantenaar, S. J. Campbell, D. H. Chaplin, and G. V. H. Wilson, J. Phys. E **10**, 825 (1977).
[45]L. B. Robinson and F. Milstein, Solid State Commun. **13**, 97 (1973).
[46]I. S. Williams, E. S. R. Gopal, and R. Street, Phys. Status Solidi **67**, 83 (1981).
[47]B. J. Beaudry and K. A. Gschneidner, Jr., in *Handbook on the Physics and Chemistry of Rare Earths,* edited by K. A. Gschneidner, Jr. and L. R. Eyring (North-Holland, Amsterdam, 1978).
[48]G. Ahlers, Rev. Mod. Phys. **52**, 489 (1980).
[49]A. Aharony and M. E. Fisher, Phys. Rev. B **27**, 4394 (1983).
[50]H. S. Kogon and A. D. Bruce, J. Phys. C **15**, 5729 (1982).
[51]P. Beauvillain, C. Chappert, and I. Laursen, J. Phys. C **13**, 1481 (1980).
[52]D. J. W. Geldart and G. Malmström, J. Phys. C **15**, 5811 (1982).
[53]R. M. Suter and C. Hohenemser, J. Appl. Phys. **50**, 1814 (1979).
[54]K. H. Mueller, G. Ahlers, and F. Pobell, Phys. Rev. B **14**, 2096 (1976).
[55]A. Kornblit and G. Ahlers, Phys. Rev. B **11**, 2678 (1975).
[56]A. Kornblit, G. Ahlers, and E. Buehler, Phys. Rev. B **17**, 282 (1978).
[57]K. D. Jayasuriya, A. M. Stewart, S. J. Campbell, and E. S. R. Gopal, J. Phys. F **14**, 1725 (1984).
[58]C. W. Garland, G. Nounesis, and K. J. Stine, Phys. Rev. A **39**,

4919 (1989).
[59]V. Privman, P. C. Hohenberg and A. Aharony, in *Phase Transitions and Critical Phenomena,* edited by C. Domb and J. L. Lebowitz (Academic, New York, 1991), Vol. 14.
[60]A. Aharony and A. D. Bruce, Phys. Rev. **10**, 2973 (1974).
[61]M.-C. Chang and A. Houghton, Phys. Rev. Lett. **44**, 785 (1980).
[62]A. Aharony and G. Ahlers, Phys. Rev. Lett. **44**, 782 (1980).
[63]A. D. Bruce, J. M. Kosterlitz, and D. R. Nelson, J. Phys. C **9**, 825 (1976).
[64]C. Bagnuls and C. Bervillier, Phys. Lett. **107A**, 299 (1985).
[65]L. D. Jennings, R. E. Miller, and F. H. Spedding, J. Chem. Phys. **33**, 1849 (1960).
[66]C. Bagnuls and C. Bervillier, Phys. Rev. B **32**, 7209 (1985).
[67]A. Singsaas and G. Ahlers, Phys. Rev. B **30**, 5103 (1984).
[68]G. Bednarz and D. J. W. Geldart, J. Phys. Condens. Matter (to be published).
[69]R. A. Cowley and K. Carneiro, J. Phys. C **13**, 3281 (1980).
[70]L. P. Kadanoff, W. Götze, D. Hamblen, R. Hecht, E. A. S. Lewis, V. V. Palciauskas, M. Rayl, and J. Swift, Rev. Mod. Phys. **39**, 395 (1967).